Applied Mathematics and Computation 219 (2013) 5113–5122

Contents lists available at SciVerse ScienceDirect

Applied Mathematics and Computation

journal homepage: www.elsevier.com/locate/amc

A survey on the integrated design of chaotic oscillators

R. Trejo-Guerra [a], E. Tlelo-Cuautle [b,*], V.H. Carbajal-Gómez [b], G. Rodriguez-Gómez [b]

[a] *SEMTECH-Snowbush Mexico Design Center, Mexico*
[b] *INAOE, Department of Electronics, Luis Enrique Erro No. 1, Tonantzintla, Puebla 72840, Mexico*

ARTICLE INFO

Keywords:
Chaotic oscillator
Electronic implementation
Integrated circuit
Multi-scroll
Chua's circuit

ABSTRACT

We present a review on the electronic design of chaotic oscillators. Multi-scroll chaotic oscillators are listed according to their electronic implementations. A 3-scrolls oscillator is analyzed from its mathematical description, and designed with current-feedback operational amplifiers. Finally, we list the integrated realizations, and discuss key points for future research on the design of multi-scroll chaotic oscillators.

1. Introduction

Electronic implementations of chaotic oscillators are relatively new and in some cases there is still mathematical research to be done. Most of the potential applications exploits the deterministic nature of chaotic signals [1,2], while others are related to the random behavior [3]. For example, the synchronization and transmission of encrypted information [4,5], show advantages based on the complexity of chaotic signals, which turns them suitable for message encryption.

It was since nineties, that much research has been oriented to implement chaotic oscillators with electronic devices. A remarkable design of a continuous chaotic oscillator is the case of the two-scroll Chua's circuit [6–10], which generates a rich variety of chaotic dynamics in a relatively simple electronic implementation. Recently, many new chaotic oscillators have been proposed [11–13]. In all cases a nonlinear part is required to obtain more equilibrium points than the origin and eventually obtain attractive regions. Some approaches use polynomial forms, sinusoidal functions, delay based functions, or piecewise-linear (PWL) functions [3,14]. In particular, the PWL-based implementations show numerous research works because of their capacity to obtain at least partial analytical solutions (for the linear segments), while the obtention of such solutions for other nonlinearities are hard to reach [3]. This motivates the development of new PWL-based chaotic oscillators showing more scrolls (multi-scroll attractors), and more directions [5,11,12,15,16].

Currently, a collection of major developments of chaotic systems can be found in [3], where several researchers summarize key guidelines on modeling, simulation, control synchronization, and applications of chaotic oscillators. Besides, although chaotic oscillators have been intensively studied since a few decades ago, their implementation using electronic devices has been considered only in a very few works. Henceforth, this survey describes the electronic implementation of theoretical chaotic oscillators using discrete active devices and integrated circuit realizations.

2. Electronic implementations of chaotic oscillators

The majority of electronic implementations of chaotic oscillators consist of discrete active devices, mainly operational amplifiers (opamps) [16], whereas other designs are implemented with mixed-mode active devices [17,18], such as the current-feedback opamp (CFOA [8,19], e.g. the Analog Devices AD844), operational transconductance amplifier (OTA) [13],

* Corresponding author.
E-mail address: etlelo@inaoep.mx (E. Tlelo-Cuautle).

0096-3003/$ - see front matter
http://dx.doi.org/10.1016/j.amc.2012.11.021

positive-type second-generation current conveyor (CCII+) [4,20], and unity–gain cells (UGCs) [10–12]. Relevant chaotic continuous-time oscillator designs are summarized in Table 1, where the following issues can be identified:

- The majority of those designs have been obtained by generalizing previous others, for example, the most preferred dynamic system is the Chua's chaotic oscillator.
- PWL-based oscillators are preferred because of the relatively simple mathematical description, dynamical analysis and circuit synthesis.
- Implementations using integrated circuit technology are few in all cases and multi-scroll designs scarce.

As one can infer, many multi-scroll chaotic oscillators are derived from the double-scroll Chua's chaotic circuit. Basically, the nonlinear resistor known as Chua's diode [8] is augmented, as shown in Fig. 1, to have more break points while combining the slopes [19,21], to generate even or odd number of scrolls. Other PWL functions can be added to implement chaotic oscillators in more than one direction (1D) [5,16], e.g. 2D [22], 3D [23], and 4D [24].

The electronic implementations of those chaotic oscillators based on PWL functions use different kinds of active devices; the most used one is the traditional opamp [2]. The CFOA AD844 from Analog Devices is also quite useful, and it can be used as CCII+ [20], as already demostrated in [3,4]. The OTA has been used to implement double-scroll chaotic oscillators in [6,7]. Those three active devices have been summarized in [13] to show the generic topologies for realizing the PWL saturated function series. From the integrated circuit design point of view, the unity-gain cells (UGCs) can be interconnected or superimposed to derive mixed-mode active devices like CCIIs and CFOAs [18]. Besides, the UGCs not only can be implemented with the CFOA AD844 [10,19], but also with integrated circuit technology [11,12].

As an example, we describe the electronic implementation of a multi-scroll Chua's chaotic oscillator using the CFOA AD844. We show the values of the Lyapunov exponents computed by applying the method described in [14,25], and its bifurcation diagram to highlight the operation in chaotic regime.

The design starts by describing the multi-scroll Chua's chaotic oscillator by (1), where $\alpha = 10,\ \beta = 11.5$ and the PWL function is represented by (2).

$$\begin{aligned} \dot{x} &= \alpha(y - x - f(x)), \\ \dot{y} &= x - y + z, \\ \dot{z} &= -\beta y, \end{aligned} \tag{1}$$

$$f(x) = m_{2n-1}x + \frac{1}{2}\sum_{i=q}^{2n-1}(m_{i-1} - m_i)(|x + b_i| - |x - b_i|), \tag{2}$$

where $q = 1$ to generate $(2n)$ even scrolls, and $q = 2$ to generate $(2n - 1)$ odd scrolls. Vector m represents the slopes of the PWL function and vector b denotes the break points [19,21]. To generate even scrolls m is taken as $[m_0 \ldots m_9] = [-4.416,$

Table 1
Electronic design techniques for chaotic oscillators.

System Name		Nonlinear function based on			Reference	
Name	Attractor type	Function	Proposed circuit	Integrated design	Author	Year
Chua's circuit	Double-scroll	PWL	Opamp, OTA, CFOA, UGC, CCII+	OTA	Chua [26], Delgado [7]	1993
	1D	PWL	Opamp		Suykens [27]	2000
	1D	Sinusoidal	Trigonometric function generator		Tang [28]	2001
	1D	PWL	Opamp		Zhong [29]	2002
	1D	PWL	FGMOS	FGMOS	Fujiwara [30]	2003
	1D, 2D	PWL (saw-tooth)	Opamp		Yu [31]	2007
Lorenz	Double-scroll	Product	Multiplier	OTA, Multiplier	González [32]	2000
	Multi-scroll	Complex	DSP		Yu [33]	2006
Third order canonical system	double scroll	PWL	CFOA,Opamp	OTA, Opamp	Elwakil [34]	2000
	1D-3D	PWL	CFOA, Opamp		Yalcin [35]	2002
	1D-3D	PWL	Opamp		Lü [36]	2004
	1D-3D	Hysteresis	Opamp, diode		Lü [2]	2006
Second order hyst.	1D, 2D	Hysteresis	Opamp, diode		Han [37]	2004
NA	1D, 2D	$tanh()$	Differential pair, OTA		Ozoguz [38]	2002
NA	double-scroll	$tanh()$	LC		Ozoguz [39]	2005
NA	1D	PWL, $tanh(), t$	CFOA, TX line		Yalcin [40]	2007
NA	double sroll	PWL	current mirror, C		Ozoguz [41]	2008

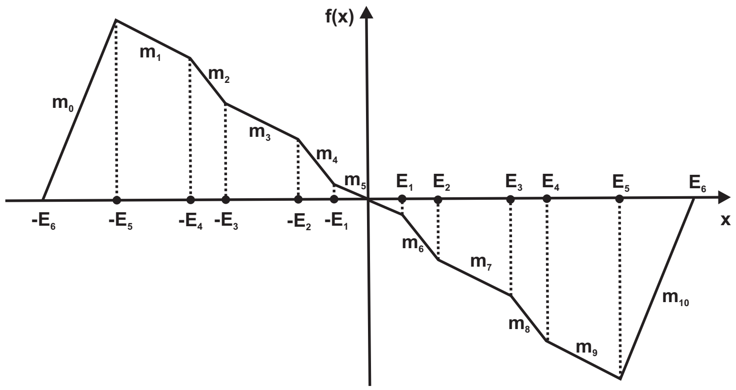

Fig. 1. PWL description of Chua's diode to generate multi-scroll attractors.

$-0.276, -3.036, -0.276, -3.036, -0.276, -3.036, -0.276, -3.036, -0.276]$ and $[b_1 \dots b_9] = [0.1, 1.1, 1.55, 3.2, 3.85, 5.84, 6.6, 8.7, 9.45]$; while to generate odd scrolls $[b_2 \dots b_9] = [0.8, 1.4, 3.2, 3.9, 5.8, 6.4, 8.3, 9.2]$.

As a particular case, we will show the analysis for the generation of 3-scrolls. According to Fig. 1, the PWL function can be decomposed in 5 regions defined by,

$$
\begin{aligned}
&D_2 = \{(x, y, z) | x \geqslant E_2\},\\
&D_1 = \{(x, y, z) | x \geqslant E_1\},\\
&D_0 = \{(x, y, z) | -E_1 \leqslant x \leqslant E_1\},\\
&D_{-1} = \{(x, y, z) | x \leqslant -E_1\},\\
&D_{-2} = \{(x, y, z) | x \leqslant -E_2\}.
\end{aligned} \tag{3}
$$

where E_i denotes a break point. In this case: E_1 and E_2 being $b_2 = 0.8$ and $b_3 = 1.4$, respectively. The nonlinear function f (x) given in (2) can now be described by its m_i slopes and b_i breakpoints as:

$$
f(x) = \begin{cases}
m_7 x + (m_5 - m_6) b_2 + (m_6 - m_7) b_3 & x \geqslant b_3,\\
m_6 x + (m_5 - m_6) b_2 & x > b_2,\\
m_5 x & -b_2 \leqslant x \leqslant b_2,\\
m_4 x + (m_4 - m_5) b_2 & x < -b_2,\\
m_3 x + (m_4 - m_5) b_2 + (m_3 - m_4) b_3 & x \leqslant -b_3.
\end{cases} \tag{4}
$$

From (1), one can compute the equilibrium points (EPs), where the static equations are given as,

$$
\begin{aligned}
&f(x) = 0,\\
&y = 0,\\
&z = -x.
\end{aligned} \tag{5}
$$

In each PWL region, $D_2, \dots, D_{-2}$, the system has a unique EP. The 5 EPs are given as,

$$
\begin{aligned}
&EP_2^+ = (k_1, 0, -k_1) \in D_2,\\
&EP_1^+ = (k, 0, -k) \in D_1,\\
&EP_0 = (0, 0, 0) \in D_0,\\
&EP_1^- = (-k, 0, k) \in D_{-1},\\
&EP_2^- = (-k_1, 0, k_1) \in D_{-2}.
\end{aligned} \tag{6}
$$

where $k = (g_2 - g_1)E_1/(g_2 + 1)$ and $k_1 = ((g_2 - g_1)E_1 + (g_1 - g_2)E_2)/(g_1 + 1)$, with $g_1 = m_3 = m_5 = m_7$ and $g_2 = m_4 = m_6$, according to (2).

The mathematical representation from (1) derives a linear expression of the form $\dot{x} = Ax + b$ [19]. The 5 regions can be denoted as:

$$
\dot{x} = \begin{cases}
A(\alpha, \beta, m_3)(x - k_1) & x \in D_2,\\
A(\alpha, \beta, m_4)(x - k) & x \in D_1,\\
A(\alpha, \beta, m_5)x & x \in D_0,\\
A(\alpha, \beta, m_6)(x + k) & x \in D_{-1},\\
A(\alpha, \beta, m_7)(x + k_1) & x \in D_{-2},
\end{cases} \tag{7}
$$

where $x = [x, y, z]^T$, $k = [k, 0, -k]^T$, $k_1 = [k_1, 0, -k_1]^T$ and the Jacobian matrix can be expressed by (8). The characteristic equation of the linearization around the equilibrium points is given by (9), where m_i is the corresponding slope for the 5 regions defined by (7).

$$[A(\alpha, \beta, m_i)] = \begin{bmatrix} -\alpha(m_i + 1) & \alpha & 0 \\ 1 & -1 & 1 \\ 0 & -\beta & 0 \end{bmatrix}, \tag{8}$$

$$\lambda = \lambda^3 + [1 + \alpha(m_i + 1)]\lambda^2 + [\beta + \alpha m_i]\lambda + \alpha\beta(1 + m_i). \tag{9}$$

The analysis of each linear region m_i is done using $\alpha = 10$, $\beta = 11.5$, $g_1 = -0.276$ and $g_2 = -3.036$, according to (2). Therefore, the computed EPs are given by

$EP_2^+ = (2.2873, 0, -2.2873) \in D_2,$
$EP_1^+ = (1.0845, 0, -1.0845) \in D_1,$
$EP_0 = (0, 0, 0) \in D_0,$
$EP_1^- = (-1.0845, 0, 1.0845) \in D_{-1},$
$EP_2^- = (-2.2873, 0, 2.2873) \in D_{-2}.$

For $m_i = g_1$ (regions D_2, D_0, D_{-2}) the Jacobian matrix from (1) at the equilibrium points $(EP_2^+, 0, EP_2^-)$ is given as:

$$\left[J(EP_2^\pm, 0)\right] = \left[\tfrac{\partial F}{\partial x}\right] = \begin{bmatrix} -7.2400 & 10.0000 & 0 \\ 1.0000 & -1.0000 & 1.0000 \\ 0 & -11.5000 & 0 \end{bmatrix}, \tag{10}$$

which has the following eigenvalues,

$\lambda_1^{EP\pm2,0} = -8.3823,$
$\lambda_2^{EP\pm2,0} = 0.0712 + 3.1508i,$
$\lambda_3^{EP\pm2,0} = 0.0712 - 3.1508i.$

For $m = g_2$ (regions D_1, D_{-1}) the Jacobian matrix from (1) at the equilibrium points (EP_1^+, EP_1^-) becomes:

$$\left[J(EP_1^\pm)\right] = \left[\tfrac{\partial F}{\partial x}\right] = \begin{bmatrix} 20.3600 & 10.0000 & 0 \\ 1.0000 & -1.0000 & 1.0000 \\ 0 & -11.5000 & 0 \end{bmatrix}, \tag{11}$$

which has the following eigenvalues,

$\lambda_1^{EP\pm1} = 20.8072,$
$\lambda_2^{EP\pm1} = -0.7236 + 3.2755i,$
$\lambda_3^{EP\pm1} = -0.7236 - 3.2755i.$

From the computed eigenvalues, those can be classified as saddle point of index 2 and saddle point of index 1, respectively.

2.1. Numerical simulation

The simulation of (1), leads us to compute the PWL function shown in Fig. 2(a), two state variables are shown in Fig. 2(b), and the 3-scrolls attractor computed using $X = [0.1, 0, 0]$ as initial conditions, is shown in Fig. 2(c).

2.2. Lyapunov exponents

The Lyapunov exponents are computed by applying the method given in [14,25]. Those exponents are related to the expansion or contraction nature of the different directions in the phase diagram. In fact, in a dissipative continuous dynamical system, the possible spectrums for the Lyapunov exponents in a third order system are: $(+, 0, -)$, strange attractor; $(0, 0, -)$, double torus; $(0, -, -)$, limit cycle; and $(-, -, -)$, fixed point [42]. In our case, the Lyapunov exponents are 0.37522, 0.0044 and -7.7984, confirming chaotic regime.

2.3. Bifurcation diagram

The bifurcation diagram is generated on the plane X–Y, as shown in Fig. 3 by varying α from 5 to 15 in steps of 0.01. The integration time was set to T = 400 for each increment in α [14]. As one sees, the chaotic behavior is present for α between 7.8 and 10.7.

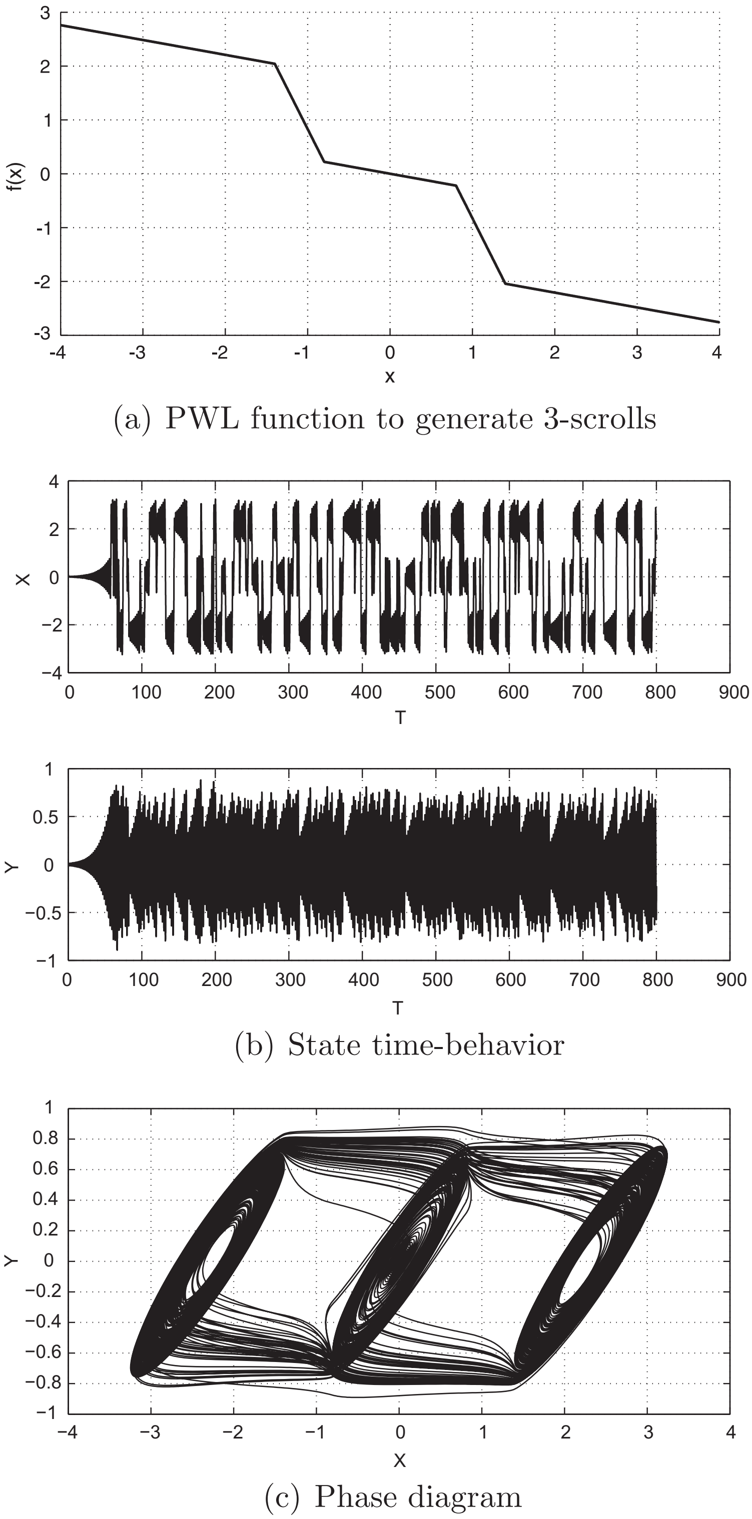

(a) PWL function to generate 3-scrolls

(b) State time-behavior

(c) Phase diagram

Fig. 2. 3-Scrolls generated from a modified Chua's circuit [19,21].

2.4. Electronic implementation using CFOAs

The multi-scroll chaotic oscillator described in this section was implemented using the CFOA AD844 [19], as shown in Fig. 4.

The values of α and β correspond to the coefficients $\frac{R_{73}}{R_{72}} = \frac{R_{73}}{R_{71}}$ and $\frac{R_{32}}{R_{31}}$, respectively. The resistances $R_{61} = R_{62}$ are tuned to adjust the gains of the PWL function, which is build by using the finite gain model of the CFOA. That way, several saturated-cells, as the one shown in Fig. 5, can be connected in parallel to synthesize the PWL function [13]. For instance, the behavior of the saturated cell shown in Fig. 5, can be described by (12).

$$V_{out}(V_{in}) = \begin{cases} \frac{R_{out}(V^- - E)}{R_x} & V_{in} < V^-, \\ \frac{R_{out}(V_{in} - E)}{R_x} & V^- < V_{in} < V^+, . \\ \frac{R_{out}(V^+ - E)}{R_x} & V_{in} > V^+, \end{cases} \quad (12)$$

To generate 3-scrolls, three saturated cells are connected in parallel as shown in Fig. 6. The values are assigned according to the procedure introduced in [19]. Fig. 7 shows the 3-scrolls attractor simulated in HSPICE using the macromodel of the CFOA AD844. Experimental results using the CFOA AD844 are shown in [3,19,43,44].

3. Integrated design of chaotic oscillators

As mentioned in the previous sections, the majority of chaotic oscillator designs have been implemented mainly by using discrete active devices, e.g. opamps in the majority of cases. Moreover, the use of practically recent mixed-mode active devices [18], with IC technology allows us to implement integrated systems, as recently demonstrated in [11,12,45]. However, still many open problems in the development of integrated chaotic oscillators, are good opportunities for future research. For instance, a brief discussion on the integrated implementations of chaotic oscillators is given below.

Cruz and Chua design: One of the first monolithic implementations was the Chua's chaotic oscillator [26]. The fabricated IC required external resistors connected between terminals 1 and 2 and between 5 and 6 of the developed chip shown by Fig. 3 in [26], with the purpose of adjusting the nonlinear function gain. That nonlinear function was generated by using two OTAs, each one with different transconductance values and labeled as A and B, and also each one with different current bias levels. The inductor was designed from the gyrator concept also using OTAs.

Rodríguez and Delgado design: A similar Chua's implementation was realized based on the state variables perspective [7] (the normalized system). Arranging identical OTAs in parallel used gm-C integrators. The nonlinear function was realized by two OTAs connected in parallel, but each one with independent bias control.

Elwakil et al. Design: The two-scroll version of the original canonical system was also realized by selecting the capacitance or resistances of the loads, as described in [34]. Thus allowing having positive and negative integrals. All the system parameters were available since all the loads were externally connected. Using an inverter as comparator made the nonlinear function.

Fujiwara et al. design: These authors proposed a circuit similar to that introduced by Cruz and Chua [26]. A simulated inductor was also used, and transistors were biased to operate in the linear region to implement the resistor [30]. A particular change was introduced in the design of the nonlinear function, which was designed using floating-gate MOS transistors

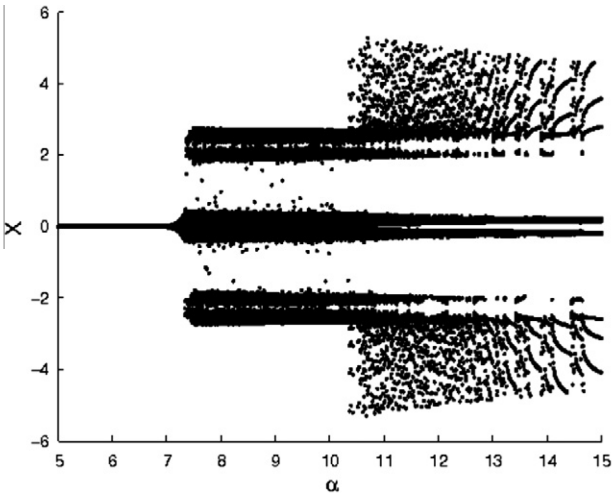

Fig. 3. Bifurcation diagram.

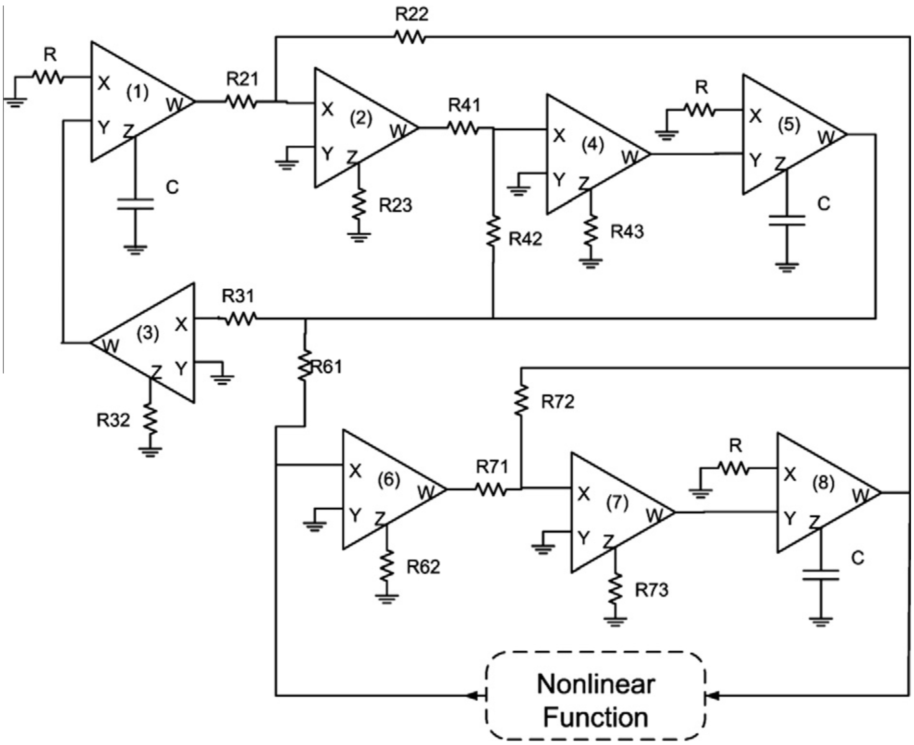

Fig. 4. Implementation using CFOAs.

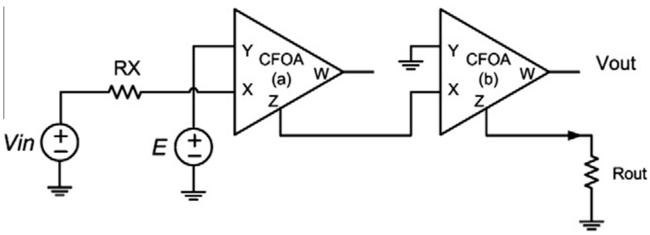

Fig. 5. CFOA-based saturated cell.

(FGMOS). The FGMOS transistors were exploited as switches in the current path. That way, the nonlinear function approached by a PWL one, allows increasing the number of linear segments by connecting several cells in parallel. The disadvantage of that design is the requirement of external controls to adjust the slope and breakpoints of the voltage-to-current (V-I) characteristic of the PWL function. The authors in [30] reported a 3-scroll experimental attractor, obtained from the introduction of the first multi-scroll chaotic oscillator, implemented with IC technology. However, the poor common-mode rejection ratio (CMRR) did not allow proving the generation of more scrolls.

Table 2 summarizes some details of these integrated chaotic oscillators, and the new one introduced by Trejo-Guerra and colleagues in [11,12]. The center frequency listed in the last row of Table 2, of 3.5 MHz was observed by using the internal capacitances, not the external ones already shown in [11,12]. Most important is that from this Table one can infer the necessity of developing novel IC designs for chaotic oscillators generating not only multi-scrolls, but also multi-scrolls in multiple directions.

Reference [11] summarizes integrated realizations of multi-scroll chaotic oscillators, and introduces a modified Chua's circuit whose PWL function is a saw-tooth one. That work shows the analysis of the dynamical system to obtain the circuit design requirements. The article proposes an innovative design using FGMOS transistors to implement a V-I PWL function to generate multi-scrolls. The experimental confirmation of that integrated design is given in [12], where the authors introduce for the first time: parameter, technology and process variation analysis. The article shows the experimental observation of 3- and 5-scrolls from the fabricated IC in technology of 0.5 μm.

Discussion on the design of chaotic oscillators using IC technology is given in [11,12]. For instance, as seen in Table 1, PWL functions allow obtaining several multi-scroll oscillator schemes. To design those functions with electronic devices, a

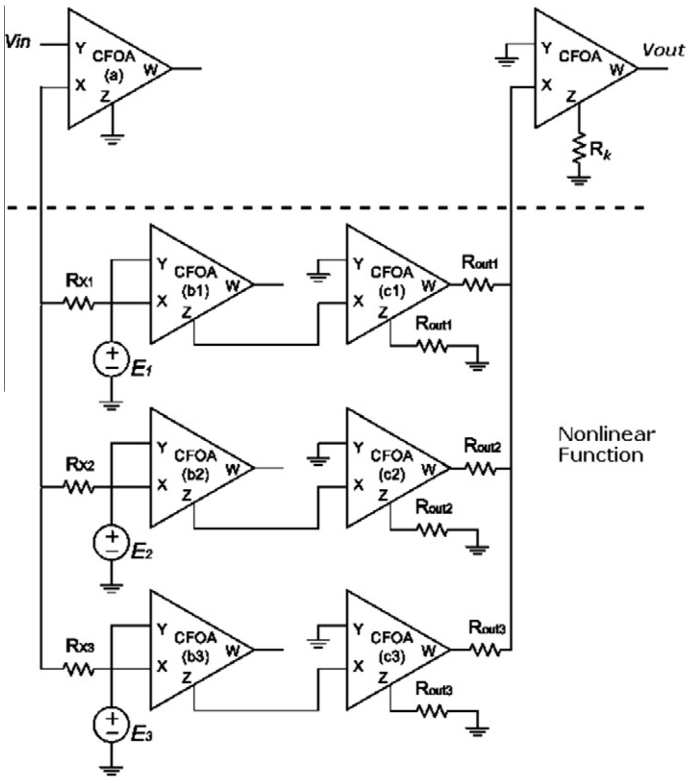

Fig. 6. PWL function implemented with saturated cells to generate 3-scrolls.

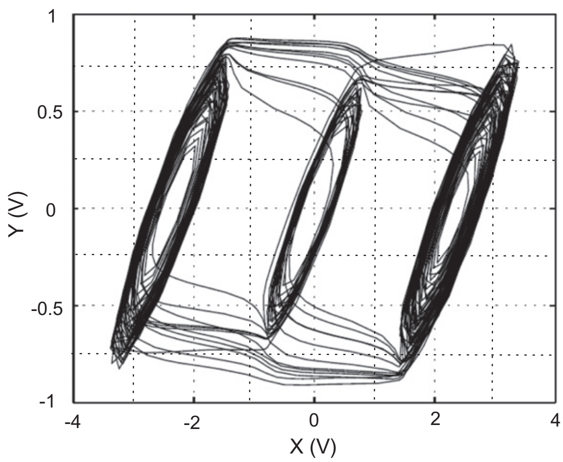

Fig. 7. Hspice simulation result.

Table 2
Chaotic oscillators implemented with CMOS IC technology.

Author	Technology	Bias Levels	Center Freq.	PWL function strategy
Cruz & Chua [26]	2 μm	–	160 kHz	Distinct bias currents and saturation
Rodríguez & Delgado [7,46]	2.4 μm	±2.5 V	–	Distinct bias currents and saturation
Elwakil et al. [34]	1.2 μm	±2.5 V	118 kHz	Simple inverter
Fujiwara et al. [30]	0.35 μm	±1.65 V	7 MHz	Switching currents FGMOS transistors
Trejo-Guerra et al. [11,12]	0.5 μm	±2.5 V	3.5 MHz	FGMOS inverter

switching component may be used. Direct applications will achieve stair-like or saw-tooth functions; also, by controlling the biasing of some linear active cell, other PWL functions can be generated. But the implementation of the nonlinear or PWL function is a challenge design issue because the behavior must be accurate to keep the relations of the dynamical system and its equilibrium points, simultaneously. It means that the design of nonlinear functions has several dimensions of difficulty compared to a simple linear design. The first problem is how to mitigate input and output offset points on PWL segments, and active function blocks performing integration, addition or subtraction operations. The slow rate affects the bandwidth capacity in different manners (according to the specific PWL function), the hysteresis effects may produce more than two different signal paths, and so on.

4. Conclusions

This article summarized recent developments on the electronic implementation of chaotic oscillators. It was focused on multi-scroll chaotic oscillators, and specifically those based on PWL functions. Several PWL-function based multi-scroll chaotic oscillators were listed and we highlighted that the majority of them are modifications of the well-known double-scroll Chua's circuit.

Key references for using active devices such as opamps, CFOAs, OTAs, CCIIs, and unity-gain cells were listed for the discrete implementation of chaotic oscillators.

A table summarizing the very few works on the integrated design of chaotic oscillators was given in the last section. As a final conclusion, we appeal performing research on the electronic implementation of multi-scroll chaotic oscillators using not only discrete active devices, but also using modern IC technologies. Interested designers can find guidelines on the IC implementation of multi-scroll chaotic oscillators based on PWL function approaches in [11,12].

Acknowledgement

This work is partially supported by CONACyT Mexico under project number 131839-Y.

References

[1] Ch.K. Volos, I.M. Kyprianidis, I.N. Stouboulos, A chaotic path planning generator for autonomous mobile robots, Rob. Auton. Syst. 60 (2012) 651–656.
[2] J. Lü, G. Chen, Generating multi-scroll chaotic attractors: theories, methods and applications, Int. J. Bifurcation Chaos 16 (4) (2006) 775–858.
[3] E. Tlelo-Cuautle, Chaotic Systems, InTech Publisher, 2011.
[4] R. Trejo-Guerra, E. Tlelo-Cuautle, C. Cruz-Hernández, C. Sánchez-López, Chaotic communication system using Chua's oscillators realized with CCII+s, Int. J. Bifurcation Chaos 19 (12) (2009) 4217–4226.
[5] J.M. Munoz-Pacheco, E. Zambrano-Serrano, O. Felix-Beltran, L.C. Gomez-Pavon, A. Luis-Ramos, Synchronization of PWL function-based 2D and 3D multi-scroll chaotic systems, Nonlinear Dyn. 70 (2) (2012) 1633–1643.
[6] M. Delgado-Restituto, A. Rodríguez-Vázquez, Design considerations for integrated continuous-time chaotic oscillators, IEEE Trans. Circuits Syst. I 45 (1998) 481–495.
[7] A. Rodríguez-Vázquez, M. Delgado-Restituto, CMOS design of chaotic oscillators using state variables: a monolithic Chua's circuit, IEEE Trans. Circuits Syst. II 40 (10) (1993) 596–613.
[8] E. Tlelo-Cuautle, A. Gaona-Hernández, J. García-Delgado, Implementation of a chaotic oscillator by designing Chua's diode with CMOS CFOAs, Analog Integr. Circuits Signal Proc. 48 (2006) 159–162.
[9] E. Tlelo-Cuautle, J.M. Muñoz-Pacheco, Numerical simulation of Chua's circuit oriented to circuit synthesis, Int. J. Nonlinear Sci. Numer. Simul. 8 (2) (2007) 249–256.
[10] C. Sánchez-López, A. Castro-Hernandez, A. Perez-Trejo, Experimental verification of the Chua's circuit designed with UGCs, IEICE Electron. Express 5 (17) (2008) 657–661.
[11] R. Trejo-Guerra, E. Tlelo-Cuautle, J.M. Jimenez-Fuentes, J.M. Muñoz-Pacheco, C. Sánchez-López, Multiscroll floating gate based integrated chaotic oscillator, Int. J. Circuit Theory Appl. (2011). http://dx.doi.org/10.1002/cta.821
[12] R. Trejo-Guerra, E. Tlelo-Cuautle, J.M. Jimenez-Fuentes, C. Sánchez-López, J.M. Muñoz-Pacheco, G. Espinosa-Flores-Verdad, J.M. Rocha-Perez, Integrated circuit generating 3- and 5-scroll attractors, Commun. Nonlinear Sci. Numer. Simul. 17 (11) (2012) 4328–4335, http://dx.doi.org/10.1016/j.cnsns.2012.01.029.
[13] J.M. Muñoz-Pacheco, W. Campos-Lopez, E. Tlelo-Cuautle, C. Sánchez-López, OpAmp-, CFOA- and OTA- based configurations to design multi-scroll chaotic oscillators, Trends Appl. Sci. Res. 7 (2) (2012) 168–174.
[14] R. Trejo-Guerra, E. Tlelo-Cuautle, J.M. Muñoz-Pacheco, C. Sánchez-López, C. Cruz-Hernandez, On the relation between the number of scrolls and the Lyapunov exponents in PWL-functions-based n-scroll chaotic oscillators, Int. J. Nonlinear Sci. Numer. Simul. 11 (11) (2010) 903–910.
[15] Z. Elhadj, A new 3-D piecewise linear system for chaos generation, Radioengineering 16 (2) (2007) 40–43.
[16] J.M. Muñoz-Pacheco, E. Tlelo-Cuautle, Electronic Design Automation of Multi-scroll Chaos Generators, Bentham Sciences Publishers Ltd, 2010, http://dx.doi.org/10.2174/97816080516561100101.
[17] E. Tlelo-Cuautle, C. Sánchez-López, E. Martinez-Romero, S.X.-D. Tan, Peng Li, F.V. Fernandez, M. Fakhfakh, Behavioral modeling of mixed-mode integrated circuits, Advances in Analog Circuits, InTech Publisher, 2011, pp. 85–108.
[18] M.A. Duarte-Villaseñor, E. Tlelo-Cuautle, L. Gerardo de la Fraga, Binary genetic encoding for the synthesis of mixed-mode circuit topologies, Circuits Syst. Signal Proc. 31 (3) (2012) 849–863.
[19] R. Trejo-Guerra, E. Tlelo-Cuautle, C. Sanchez-Lopez, J.M. Munoz-Pacheco, C. Cruz-Hernandez, Realization of multi-scroll chaotic attractors by using current-feedback operational amplifiers, Rev. Mex. Fis. 56 (4) (2010) 268–274.
[20] C. Sanchez-Lopez, R. Trejo-Guerra, J.M. Munoz-Pacheco, E. Tlelo-Cuautle, N-scroll chaotic attractors from saturated functions employing CCII+s, Nonlinear Dyn. 61 (1-2) (2010) 331–341.
[21] C. Sanchez-Lopez, E. Tlelo-Cuautle, Multi-scroll chaotic oscillator employing UGCs, IEEE CONIELECOMP, Puebla, Mexico, February 2009, pp. 189–191.
[22] J.M. Munoz-Pacheco, E. Tlelo-Cuautle, Automatic synthesis of 2D-n-scrolls chaotic systems by behavioral modeling, J. Appl. Res. Technol. 7 (1) (2009) 5–14.
[23] T. Zhou, G. Chen, Classification of chaos in 3-D autonomous quadratic systems-I. Basic framework and methods, Int. J. Bifurcation Chaos 16 (9) (2006) 2459–2479.

[24] J.E. Varrientos, E. Sanchez-Sinencio, A 4-D chaotic oscillator based on a differential hysteresis comparator, IEEE Trans. Circuits Syst. I-Fundam. Theor. Appl. 45 (1) (1998) 3–10.
[25] Luis G. de la Fraga, E. Tlelo-Cuautle, V.H. Carbajal-Gomez, On maximizing positive Lyapunov exponents in a chaotic oscillator with Heuristics, Rev. Mex. Fis. 58 (3) (2012) 274–281.
[26] J.M. Cruz, L.O. Chua, An IC chip of Chua's circuit, IEEE Trans. Circuits Syst. II 40 (10) (1993) 614–625.
[27] M.E. Yalcin, J.A.K. Suykens, J. Vandewalle, Experimental confirmation of 3- and 5-scroll attractors from a generalized Chua's circuit, IEEE Trans. Circuits Syst. 47 (3) (2000) 425–429.
[28] K.S. Tang, G.Q. Zhong, G. Chen, K.F. Man, Generation of n-scroll attractors via sine function, IEEE Trans. Circuits Syst. I 48 (2001) 1369–1372.
[29] G. Zhong, K.F. Man, G. Chen, A systematic approach to generating n-scroll attractors, Int. J. Bifurcation Chaos 12 (12) (2002) 2907–2915.
[30] T. Fujiwara, Y. Horio, K. Aihara, An integrated multi-scroll circuit with floating-gate Mosfets, Proc. IEEE Int. Symp. Circuits Syst. (ISCAS) (2003) 180–183.
[31] S. Yu, W.K.S. Tang, G. Chen, Generation of nxm-scroll attractors under a Chua-circuit framework, Int. J. Bifurcation Chaos 17 (11) (2007) 3951–3964.
[32] O.A. Gonzlez, G. Han, J. Pineda de Gyvez, E. Sanchez-Sinencio, Lorenz-based chaotic Cryptosystem: a monolithic implementation, IEEE Trans. Circuits Syst. I 47 (8) (2000) 1243–1247.
[33] S. Yu, J. Lu, W.K.S. Tang, G. Chen, A general multi-scroll Lorenz system and its realization via digital signal processors, Chaos Interdisciplinary J. Nonlinear Sci. 16 (3) (2006) 033126.
[34] A.S. Elwakil, K.N. Salama, M.P. Kennedy, A system for chaos generation and its implementation in monolithic form, Proc. ISCAS (2000) 217–220.
[35] M.E. Yalcin, J.A.K. Suykens, J. Vandewalle, Families of scroll grid attractors, Int. J. Bifurcations Chaos 12 (1) (2002) 23–41.
[36] J. Lü, G. Chen, X. Yu, H. Leung, Design and analysis of multi-scroll chaotic attractors from saturated function series, IEEE Trans. Circuits Syst. 51 (12) (2004) 2476–2490.
[37] F. Han, Multi-scroll chaos generation via linear systems and Hysteresis function series, Ph.D thesis, RMIT University, Melbourne, Australia 2004.
[38] S. Ozoguz, A.S. Elwakil, K.N. Salama, N-scroll chaos Generator using nonlinear transconductor, Electron. Lett. 38 (14) (2002) 685–686.
[39] S. Ozoguz, O. Ates, A.S. Elwakil, An integrated circuit chaotic oscillator and its application for high speed random bit generation, IEEE Proc. ISCAS (2005) 4345–4348.
[40] M.E. Yalcin, S. Özoguz, n-scroll chaotic attractors from a first-order time-delay differential equation, Chaos 17 (3) (2007) 033112.
[41] A.S. Demirkol, S. Ozoguz, V. Tavas, S. Kilinc, CMOS realization of a double-scroll chaotic circuit and its application to random bit number generation, IEEE Proc. ISCAS (2008) 2374–2377.
[42] A. Wolf, J. Swift, H. Swinney, J. Vastano, Determining Lyapunov exponents from a time series, Physica (1985) 285–317.
[43] E. Tlelo-Cuautle, Analog Circuits: Applications, Design and Performance, NOVA Science Publishers Inc., 2012.
[44] V.H. Carbajal-Gomez, E. Tlelo-Cuautle, R. Trejo-Guerra, C. Sanchez-Lopez, J.M. Munoz-Pacheco, Experimental synchronization of multi-scroll chaotic attractors using current-feedback operational amplifiers, nonlinear science letters B: chaos, Fractal Synchronization 1 (1) (2011) 37–42.
[45] R. Trejo-Guerra, E. Tlelo-Cuautle, J.M. Munoz-Pacheco, C. Cruz-Hernandez, C. Sanchez-Lopez, Operating characteristics of MOSFETs in chaotic oscillators, in: Benjamin M. Fitzgerald (Ed.), Transistors Types, Materials and Applications, NOVA Science Publishers Inc., 2010, pp. 97–118.
[46] M. Delgado-Restituto, A. Rodríguez-Vázquez, Design considerations for integrated continuous-time chaotic oscillators, IEEE Trans. Circuits Syst. I 45 (1998) 481–495.